Int. J. Heat Mass Transfer. Vol. 29, No. 5, pp. 713–723, 1986
Printed in Great Britain

0017–9310/86 $3.00 + 0.00
Pergamon Journals Ltd.

Free convection in a vertical, porous annulus with constant heat flux on the inner wall—experimental results

V. PRASAD,* F. A. KULACKI†‡ and A. V. KULKARNI†

* Department of Mechanical Engineering, Columbia University, New York, NY 10027, U.S.A.
† Department of Mechanical and Aerospace Engineering, University of Delaware, Newark, DE 19716, U.S.A.

(*Received* 10 *December* 1984 *and in final form* 11 *November* 1985)

Abstract—Steady-state natural convection in a concentric, tall, vertical annulus filled with saturated, porous media is experimentally studied when the inner wall is heated by applying a constant heat flux and the outer wall is isothermally cooled. Temperature profiles and heat transfer rates are obtained for two sets of aspect and radius ratios, $A = 14.4, \kappa = 3.5$ and $A = 11.08, \kappa = 14$. The use of several solid–fluid combinations indicates a divergent behavior by Nusselt vs Rayleigh number curves, as also reported by previous investigators. An analysis of present and previous experimental data shows that the Nusselt number for a given Rayleigh number decreases as the ratio of solid and fluid thermal conductivities increases and vice versa.

1. INTRODUCTION

NATURAL convection in vertical, concentric annuli filled with saturated, porous media is a topic of several recent investigations owing to its importance in various technological applications, such as proposed burying of long, slender canisters containing high-level nuclear waste material in either deep-ocean seabed sediments or deep-earth rock layers, insulation of high temperature, gas-cooled reactor vessels, burying of drums containing heat generating chemicals in the earth and fibrous insulation of vertical pipes carrying hot or cold fluids.

Studies reported thus far, are due to Hickox and Gartling [1], Havstad and Burns [2], Philip [3], Reda [4], Prasad [5], Prasad and Kulacki [6, 7], and Prasad *et al.* [8]. The works by Hickox and Gartling [1], and Havstad and Burns [2] are both theoretical, and consider an isothermally heated annulus whose outer wall is cooled at a constant temperature, the top and bottom walls being insulated. By using a finite-element numerical scheme, Hickox and Gartling [1] have obtained results for $2 \leqslant A \leqslant 8$, $2 \leqslant A(\kappa-1) \leqslant 8$ and $Ra^* \leqslant 100$. Havstad and Burns [2] have studied the problem for $0.5 \leqslant [A(\kappa-1)] \leqslant 20$, $1 < \kappa < 10$ and $35 \leqslant [Ra^* \kappa/(\kappa-1)] \leqslant 150$ by employing three different techniques: numerical methods, perturbation techniques, and an approximate analysis. The work of Philip [3] is also analytical and is applicable for very low Rayleigh numbers.

Prasad and Kulacki [6, 7] have studied the problem via finite differences and have reported the results for $1 \leqslant A \leqslant 20$ and $1 \leqslant \kappa \leqslant 26$ [6], and for $0.3 \leqslant A \leqslant 1$ and $1 \leqslant \kappa \leqslant 11$ [7], both for $Ra^* \leqslant 10^4$. Major findings of these investigations are that the curvature effects diminish the centro-symmetric behavior of the temperature and flow fields observed in the case of cavity ($\kappa = 1$), stabilize the multi-cellular flow behavior of the shallow cavity [9], and produce a lower effective sink temperature for the thermal boundary layer on the heated wall. The Nusselt number on the inner wall thus increases with the radius ratio, but the slope of $\ln(Nu)$ vs $\ln(\kappa)$ curve decreases as κ increases. The heat transfer rate for an annulus thus asymptotically approaches that for a cylinder embedded in an infinite medium (at T_o) as κ is increased. The effects of the Rayleigh number and aspect ratio are very similar to those reported for vertical cavities and has lead to the conclusion [6] that the vertical cavity is a specific case of the annulus ($\kappa = 1$).

Reda [4] has conducted the experiments for a water–glass ($d = 320 \pm 75$ μm) filled, vertical annulus of $A = 4.25$ and $\kappa = 23$, when the inner wall is heated by applying a constant heat flux, and has reported the temperature distributions and heat transfer results for Rayleigh numbers up to 80.

A series of experiments on isothermally heated, vertical annuli has been reported by Prasad and his co-workers [5, 7, 8]. The later two studies [7, 8] are for $\kappa = 5.338$ and $A = 0.545$, 1 and 1.46, and have been conducted for various solid–fluid combinations, such as glass–water, glass–heptane, glass–glycol and steel–water. Prasad [5] has also reported the experimental results for $\kappa = 1.94$ and $A = 5.33$. These experimental data support most of the conclusions derived from the theoretical studies [1–7].

The purpose of the present work is to study experimentally the free convective heat transfer in tall annular enclosures for mixed thermal boundary conditions; the inner surface heated by applying a constant heat flux and the outer surface isothermally cooled. Using glass beads 3 and 6 mm in diameter and chrome-steel beads 6.35 mm in diameter as solid particles and water, heptane and ethylene glycol as saturating liquids, experiments have been conducted for $A = 14.4$, $\kappa = 3.5$ and $A = 11.08$, $\kappa = 14$.

‡Present address: Office of the Dean, College of Engineering, Colorado State University, Fort Collins, CO 80523, U.S.A.

NOMENCLATURE

A aspect ratio, L/D
C specific heat of fluid at constant pressure [J kg^{-1} K^{-1}]
d diameter of solid beads [m]
D annular gap width, $r_o - r_i$ [m]
g acceleration due to gravity [m s^{-2}]
k_m stagnant thermal conductivity of porous medium [W m^{-1} K^{-1}]
K permeability of porous medium equation (1) [m^2]
L height of porous medium [m]
Nu average Nusselt number on the inner wall
$\overline{Nu}$ average Nusselt number for annulus, $Q_{convection}/Q_{conduction}$, equation (5)
Pr^* Prandtl number, $\rho Cv/k_m$
q heat flux (input) on inner wall [W m^{-2}]
Q heat transfer rate [W]
r, z cylindrical polar coordinates [m]
R dimensionless radial distance, $(r-r_i)/D$
Ra^* Rayleigh number based on mean temperature difference, $g\beta KD(T_{m,i}-T_o)/(v\alpha)$
$\overline{Ra^*}$ Rayleigh number based on heat flux, equation (2)
T temperature [K]
ΔT mean temperature difference, $T_{m,i}-T_o$ [K]
T_m mean temperature on inner wall [K]
Z dimensionless axial distance, z/L.

Greek symbols
α thermal diffusivity of porous medium based on k_m, $k_m/\rho C$ [m^2 s^{-1}]
β isobaric coefficient of thermal expansion of fluid [K^{-1}]
ε porosity
θ dimensionless temperature, $(T-T_o)/(qD/k_m)$
κ radius ratio, r_o/r_i
v kinematic viscosity of fluid [m^2 s^{-1}]
ρ density of fluid [m^3 kg^{-1}].

Subscripts
f fluid
i inner wall (heated)
o outer wall (cold)
m based on stagnant thermal conductivity, k_m
s solid.

2. EXPERIMENTAL APPARATUS AND PROCEDURE

The major components of the experimental apparatus are the outer cylinder, the heater rod, the end plates, the rod guides, the cooling coil and the power supply with associated controls and instrumentation. A schematic of the apparatus is presented in Fig. 1, and a detailed description is given in ref. [10].

The inner cylinder is a cartridge heater with an effective heating length of 457 mm and is designed to provide uniform electrical power. Unheated sections of appropriate length are provided at the top and bottom so that the heating is applied only in the test section. This eliminates, to a large extent, undesired heat conduction from the portions of the heater rod protruding beyond the end planes of the porous matrix. By using two different heater rods, 25.4 and 6.35 mm in diameter, radius ratios of 3.5 and 14 are obtained in the present experiments. The corresponding aspect ratios are 14.4 and 11.08. The heater rod comprises a nickel–chromium wire wound around a magnesium oxide core with a thin sheath of incloy. Power is supplied to the heater through two Variacs in series with a voltage stabilizer, which provides reasonably accurate power control.

A brass cylinder (88.9 mm I.D. × 6.35 mm) is used as an outer cylinder for the annulus. A copper tube is wrapped and soldered around the outer cylinder through which the cooling water is circulated at a constant temperature. This provides an isothermal outer surface for the annulus. In general, the cooling water is maintained within ± 1°C of the room temperature by supplying water from a constant temperature circulator with a control accuracy of ± 0.025°C.

Insulating plates made of 31.75-mm-thick phenolite laminated plastic sheet ($k_s = 0.293$ W m^{-1} K^{-1}) are used as the end plates. These are bolted to the circular brass flanges soldered to the outer cylinder at each end. The bottom plate is squared in shape and can be rigidly mounted on a wooden base. A rod guider in the bottom plate keeps the heater rod properly aligned.

To measure the temperature at various locations, 30 gauge copper–constantan thermocouples are used with e.m.f.s. recorded by a Keithley digital multimeter of ± 1 μ V resolution (± 0.025°C). Several thermocouples are mounted on the heater rod (seven in the case of the 25.4-mm-diam. rod and nine for the 6.35-mm-diam. rod) by using plastic steel as an adhesive. Thermocouples on the outer wall are mounted by drilling blind holes in the cylinder wall. Several thermocouples are also provided on each side of the top and bottom plates to estimate the conduction heat loss through these plates.

To produce saturated, porous media, 3- and 6-mm-diam. glass beads and 6.35-mm-diam. chrome-steel beads are used as solid particles with water, heptane and ethylene glycol as saturating liquids. By using a

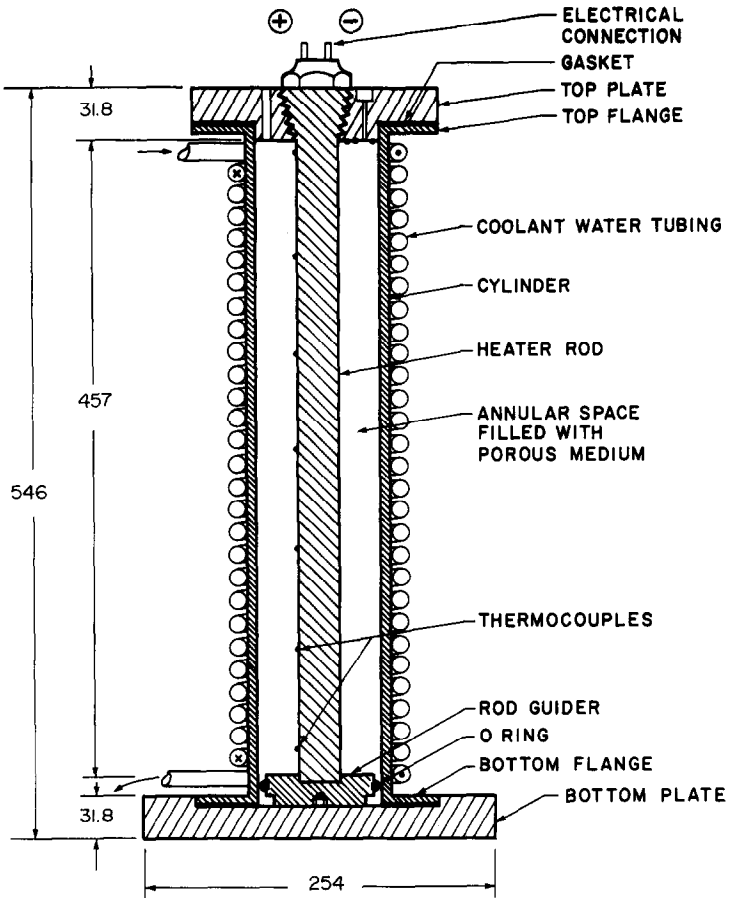

FIG. 1. Schematic cross-sectional view of the experimental apparatus (all dimensions are in millimeters).

measured amount of solid beads to fill the annulus, the porosity of the medium, ε, is obtained by calculating the volume of solid particles and the total volume. The permeability of the working medium is then calculated by using the Kozeny–Carman equation [11]:

$$K = \frac{d^2}{180}\frac{\varepsilon^3}{(1-\varepsilon)^2}. \quad (1)$$

The stagnant thermal conductivity of the porous matrix, k_m, is obtained from a correlation of Yagi *et al.* [12]. A comparison between the measured thermal conductivity for a horizontal, porous layer and the estimated value, by using the correlation, shows that the correlation predicts reasonable values for k_m [13]. Also, the correlation [12] was obtained based on the radial heat transfer in saturated, porous media, and is, thus, expected to predict reasonable values of k_m in the present case.

The Rayleigh number based on the heat flux is defined as

$$\overline{Ra^*} = \rho g C \beta K q D^2/\nu k_m^2. \quad (2)$$

Based on the mean temperature difference, $(T_{m,i} - T_o)$, the average Nusselt number on the inner surface is given by:

$$Nu = qD/(T_{m,i} - T_o)k_m. \quad (3)$$

A Rayleigh number based on the temperature difference can then be obtained as:

$$Ra^* = \overline{Ra^*}/Nu. \quad (4)$$

All the properties in equations (2) and (3) are evaluated at the mean temperature of the medium, $(T_{m,i} + T_o)/2$.

3. LOSSES AND ERRORS

The energy loss associated with the present experimental apparatus is due to the conduction through the top and bottom end plates and the axial conduction through the heater rod. As noted earlier, the temperatures are recorded on both sides of the end plates to estimate conduction losses. For the trial runs, the loss through the bottom plate has been estimated to be always less than 0.5% of the power input. This is consistent with the observation that a thick, cold layer exists in the bottom region of an annulus [6]. This loss has, thus, been neglected in calculating the net power input.

To minimize the conduction loss through the exposed surfaces of the heater rod and the top plate, the top end of the annulus is covered with a thick layer of insulating material. However, the energy lost at this end

has been estimated to be 1–7% of the power input and has been properly accounted for.

The Rayleigh and Nusselt numbers are subject to the experimental errors because of uncertainties in the quantities used to calculate these numbers, e.g. thermophysical properties of the test fluids and solids, geometric dimensions, temperature, power measurements. The uncertainty in the thermophysical properties is estimated at approximately 2% on the basis of differences in the values found in the literature. The error in the temperature measurement is about 1.5% whereas the uncertainty in the measurement of power input is approximately 1%. The linear dimensions are assumed to be accurate to 1%. Based upon these values, the uncertainty in the Rayleigh and Nusselt numbers is 6.5 and 5.5%, respectively [10].

In calculating the above uncertainties, the following sources have not been considered: (a) the inhomogeneity and anisotropy of the porous medium; and (b) the inaccuracy of the empirical relations used for calculating the permeability, K, and the stagnant thermal conductivity, k_m. There is no way by which the inhomogeneity and anisotropy of the medium can be tested. With a filling procedure, in which the fluid and the solid beads are poured alternately for a small height, and the annulus is shaken to allow proper settling each time, it is assumed that the medium has always been homogeneous and isotropic. The permeability has been calculated by using the Kozeny–Carman equation (1) for spherical balls. The error introduced in the Rayleigh number by using the above equation depends on the accuracy of the correlation itself and is well-explained in the literature [11]. However, the recent experimental data of Catton [14] indicates that the permeabilities measured by him are within 8% of the calculated values [equation (1)] for three out of four cases. In the fourth case, the variation is about 20%. The error associated with the correlation for k_m is reported in ref. [12].

Depending on the power input, the Rayleigh number and the solid–fluid combinations, a small variation of temperature on the outer wall is possible. The largest variation is about 5% of the temperature difference, $T_{m,i} - T_o$, and is observed at high Rayleigh numbers.

4. RESULTS AND DISCUSSION

As noted earlier, the experiments were conducted for two sets of aspect and radius ratios. The combination of solid and fluid, the temperature difference and the Rayleigh number range covered in each case are listed in Table 1 (the porosity and permeability of the porous medium for each set of experiments are reported in Figs. 4 and 5). The Prandtl number range covered in the present experiments is $0.2 < Pr^* < 100$.

The present results are also compared with the numerical predictions obtained for an annulus heated by a constant heat flux on the inner wall, by using the finite-difference numerical scheme described in refs. [6, 7]. For the computational results, the outer wall has been assumed to be isothermally cooled, whereas the top and bottom have been considered as adiabatic. It may be noted that the mathematical formulation used in refs. [6, 7] is valid for the porous medium obeying Darcy's law.

4.1. *Temperature distributions*

The recorded temperatures for the inner (heated) wall are presented in Figs. 2a–d and 3a,b in terms of the dimensionless temperature, θ, along with the numerically obtained temperature profiles for reasonably close values of $\overline{Ra^*}$. Though the theoretical prediction (based on Darcy's law) is for a unique temperature distribution on the inner wall for any given values of $\overline{Ra^*}$, A and κ, the experimental results indicate that the temperature is a strong function of the solid–fluid combinations besides these parameters. Qualitatively, a similar influence of the solid–fluid combination on the temperature field has also been reported by the previous investigators for vertical cavities [15] and annuli [8].

On the bottom portion of the inner wall, recorded temperatures are generally lower than the predicted values (Figs. 2 and 3). The only exception is for the case of steel–heptane when $\overline{Ra^*} = 10{,}000$ and $\kappa = 14$ (Fig. 3b). This reduction in temperature in the lower region of the annulus is primarily due to the conduction loss through the bottom plate. However, the difference

Table 1. Range of experimental data and solid–fluid combinations

Set No.	Radius ratio, κ	Aspect ratio, A	Liquid	Solid	Bead diam., d (mm)	ΔT^* (°C) min.	ΔT^* (°C) max.	$\overline{Ra^*}$ range min.	$\overline{Ra^*}$ range max.	Ra^* range min.	Ra^* range max.
1			water	glass	6	1.27	30.98	55.5	14,050	22.5	1280
2			water	glass	3	1.87	32.73	16.2	1473	6.6	290
3	3.5	14.4	glycol	glass	6	2.40	19.86	14.0	171	5.3	62
4			heptane	glass	6	1.99	21.44	983	33,159	218	2620
5			water	steel	6.35	2.38	29.23	21.3	1130	8.8	308
6			water	glass	6	3.60	37.03	338	27,665	72.7	1591
7			water	glass	3	3.98	45.22	104	4551	18.0	490
8			heptane	glass	6	5.20	23.98	7035	68,337	587	2996
9	14.0	11.08	water	steel	6.35	2.95	31.33	62.8	1681	15.1	307
10			heptane	steel	6.35	2.97	36.04	509	11,614	111	1295

* Mean temperature difference across the annulus, $(T_{m,i} - T_o)$.

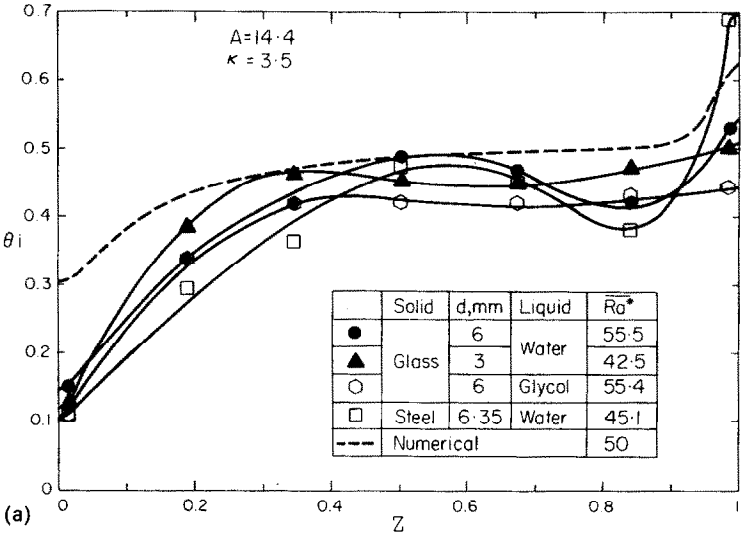

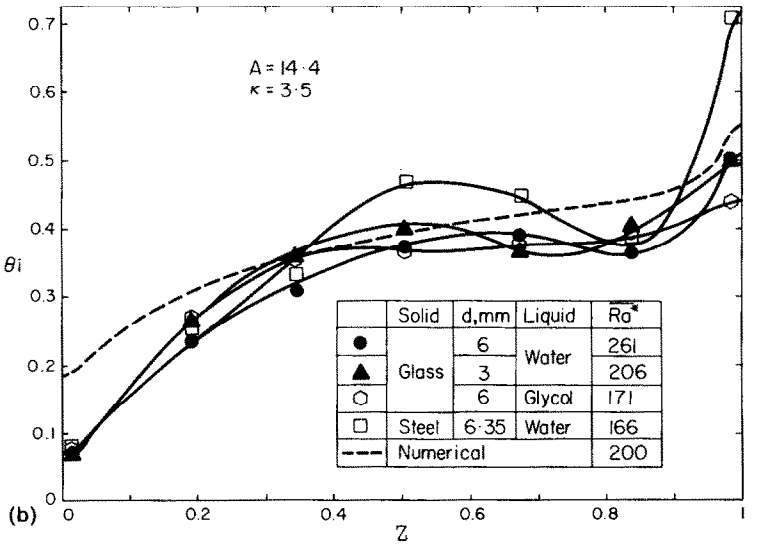

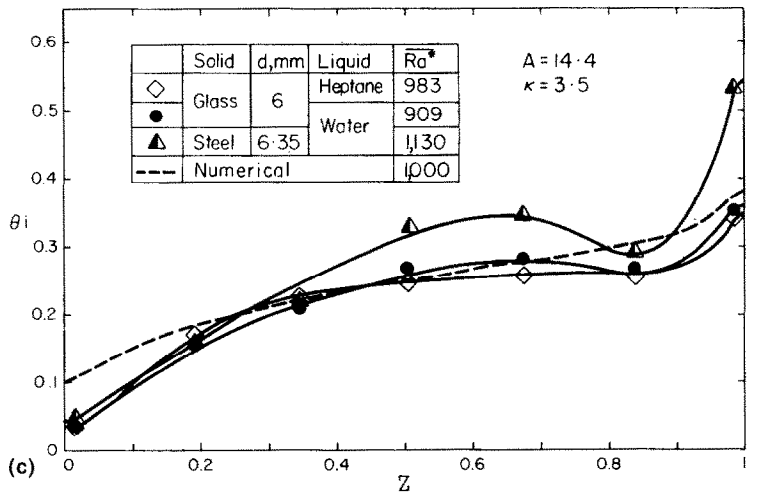

FIG. 2. Temperature distributions on the inner (heated) wall for $A = 14.4$ and $\kappa = 3.5$, for (a) $\overline{Ra^*} \simeq 50$, (b) $\overline{Ra^*} \simeq 200$, (c) $\overline{Ra^*} \simeq 1000$, and (d) $\overline{Ra^*} \simeq 10{,}000$.

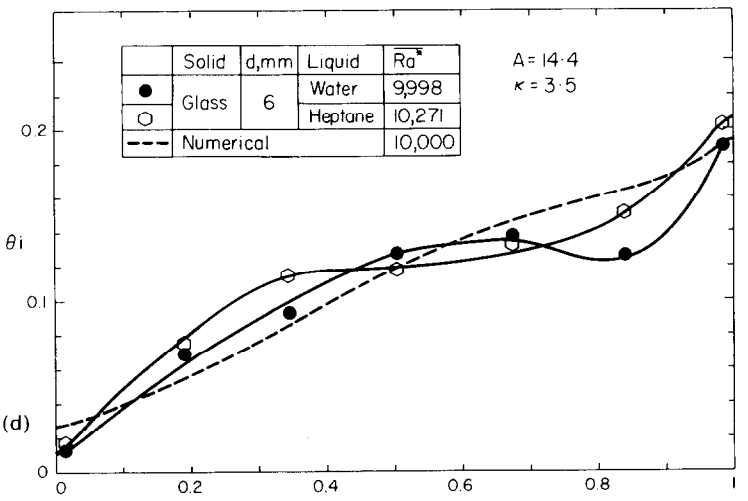

FIG. 2—*continued*

between the recorded and predicted values of θ at the first thermocouple location diminishes as the Rayleigh number is increased. At high $\overline{Ra^*}$, the temperature in the bottom region of the annulus has significantly decreased. This results in a reduction of the fraction of energy lost by conduction at the bottom wall (Figs. 2a–d).

The predicted temperature profiles further indicate that θ_i increases with height, the rate of increase being a function of $\overline{Ra^*}$ (Figs. 2 and 3). The higher the Rayleigh number, the larger is the temperature gradient $\partial\theta_i/\partial Z$—except for small distances from the top and bottom edges. In these regions, the imposed adiabatic boundary conditions result in a modified behavior. Clearly, the recorded temperatures do not follow this trend for the entire wall.

In Figs. 2a–d, measured temperatures are presented for $\overline{Ra^*} \cong 50$, 200, 1000 and 10,000 when $\kappa = 3.5$ and $A = 14.4$. At the first thermocouple location, the temperatures for various porous media are close to each other. At the second and third thermocouple locations, these temperatures are observed to vary substantially depending on the solid–fluid combinations (Figs. 2a, b). In Fig. 2a, the temperatures for water–steel are lower than those for water–glass or glycol–glass when $Z < 0.4$. The data of Figs. 2b and c exhibit a similar behavior. It may be noted that the temperatures for water–glass ($d = 6$ mm) medium are lower than those for water–steel primarily because the Rayleigh numbers for these two sets of data are not close, i.e. $\overline{Ra^*} = 261$ and 166, respectively. It is also evident from the numerical results that θ_i at any location decreases with an increase in $\overline{Ra^*}$ for a large portion of the annulus.

Consistent with the theoretical predictions, θ_i in the lower region ($Z < 0.4$) increases with Z, but the rate of increase strongly depends on the constituents of the porous medium (Figs. 2a–d). At upper locations ($Z > 0.4$), the temperature gradient, $\partial\theta_i/\partial Z$, starts decreasing and finally, reaches zero at some point. This location for zero gradient is a function of the solid–fluid combination and is observed to depend on k_s/k_f. Beyond this point, the temperature is observed to decrease which indicates a negative slope. This decrease in temperature and its extent strongly depend on the solid–fluid combinations. A water–steel medium exhibits a much sharper rise and fall compared to a water–glass or a glycol–glass medium (Figs. 2a–c). However, in a region close to the top edge, the temperature always increases and attains a peak value at $Z = 1$. Except for the water–steel medium, the recorded temperatures at the topmost thermocouples location are, in general, lower than the predicted values.

The anomalous temperature distribution in the upper region was a matter of great concern while the experiments were being conducted. The heater rods were thus properly tested for cold spots and poor thermocouple attachments. Both the heater rods were placed in ambient air and the temperatures were recorded for various power inputs. Furthermore, the rise and fall in temperatures on the inner wall do not exist for only one rod, but are observed for both the experimental set-ups (Figs. 2 and 3, and ref. [10]). Also, the negative temperature gradient, $\partial\theta_i/\partial Z$, is exhibited by more than one thermocouple reading, which establishes varying trends for different porous media. All of these strongly indicate that the present temperature distributions are not caused by some manufacturing defects.

To the authors' knowledge, there is nothing available in the literature which can support the present behavior of the recorded temperature. Except for the work of Reda [4], no other experimental work has been reported for either verical cavities or annuli with constant heat flux. In Reda's experiment, the temperatures were recorded only inside the porous medium, away from the heated wall. It seems reasonable to conclude that the present complex behavior of the inner wall temperature is a result of the combined effects of the solid–fluid combination, the curvature, the high porosity and permeability near the wall and the property variations. The present

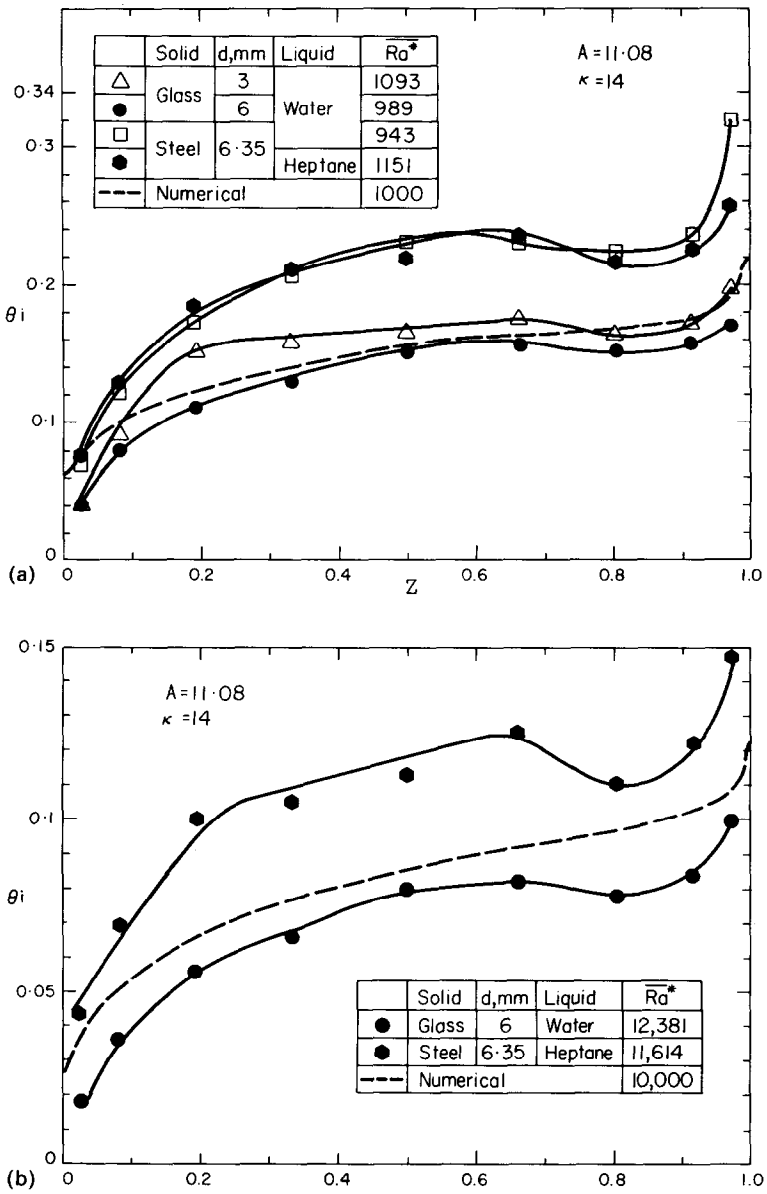

FIG. 3. Temperature distributions on the inner (heated) wall for $A = 11.08$ and $\kappa = 14$, for (a) $\overline{Ra^*} \simeq 1000$ and (b) $\overline{Ra} \simeq 10{,}000$.

experimental data and the information available in the literature are not sufficient to provide any quantitative conclusions regarding these effects.

Another interesting aspect of the temperature distributions is that the temperatures for water–glass are much closer to the theoretical prediction than the water–steel or heptane–steel temperatures. The implication is that the numerical predictions and the experimental data are closer when k_s/k_f is close to unity, but they start deviating from each other as the difference between the two conductivities increases. A similar conclusion can be derived from the experimental results of Prasad *et al.* for isothermally heated, vertical annuli [8], Seki *et al.* for vertical cavities [15], and Combarnous for horizontal layers [16].

4.2. *Heat transfer results*

Heat transfer rates are presented in Figs. 4 and 5 for $\kappa = 3.5$, $A = 14$ and $\kappa = 14$, $A = 11.08$, respectively. The Nusselt numbers plotted in these figures are based on the heat transfer coefficient on the inner wall [equation (3)], and can be used to obtain the Nusselt number as a ratio of convection to conduction heat transfer by using a relation:

$$\overline{Nu} = Nu \ln(\kappa)/(\kappa - 1). \tag{5}$$

The Nusselt number defined by equation (3) has been preferred because it allows the vertical annulus to be treated as an extension of the two-dimensional, rectangular cavity, where an additional geometric parameter κ needs to be considered [6–8].

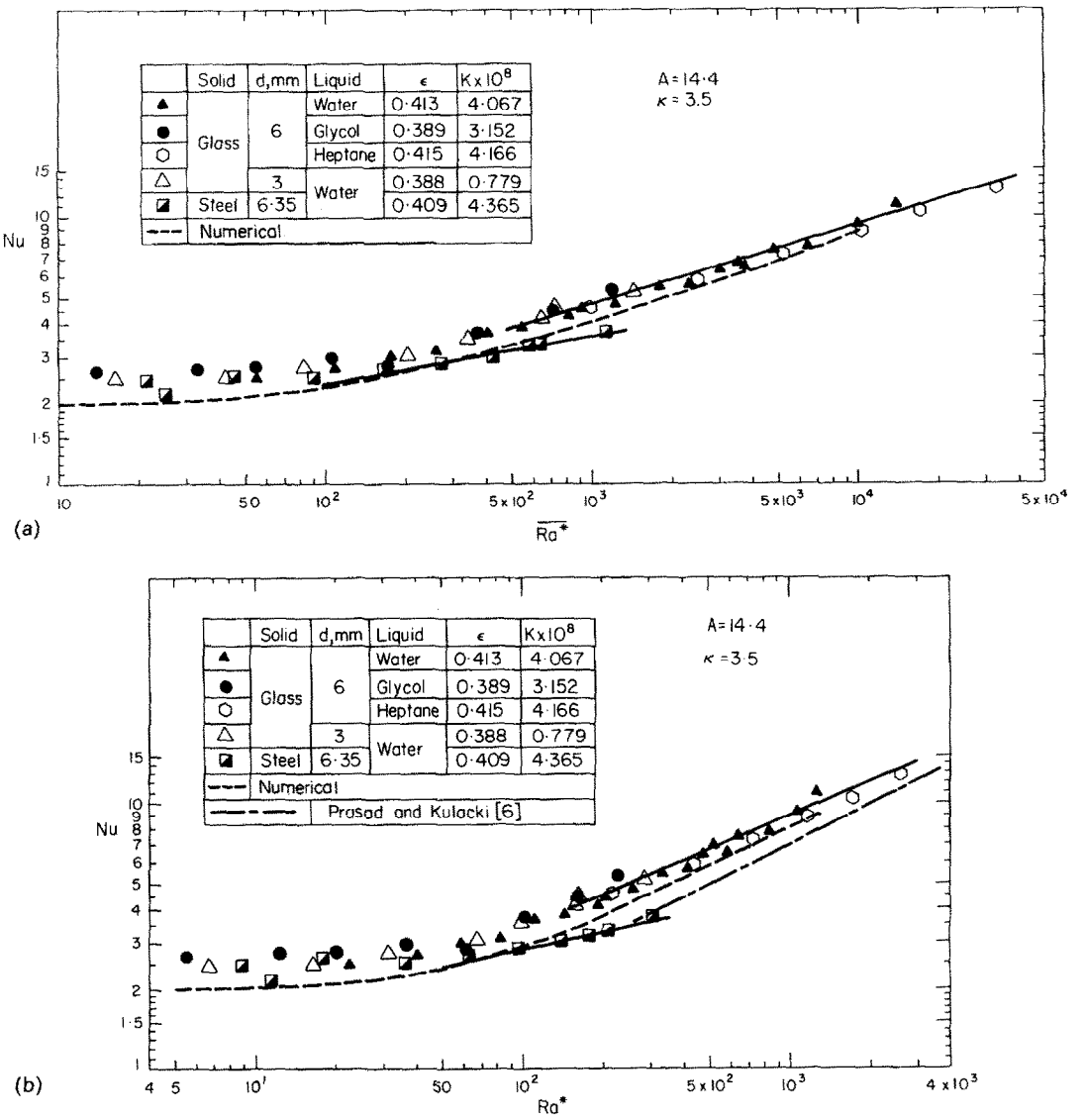

FIG. 4. Heat transfer rates for $A = 14.4$ and $\kappa = 3.5$, (a) Rayleigh number based on heat flux and (b) Rayleigh number based on mean temperature difference.

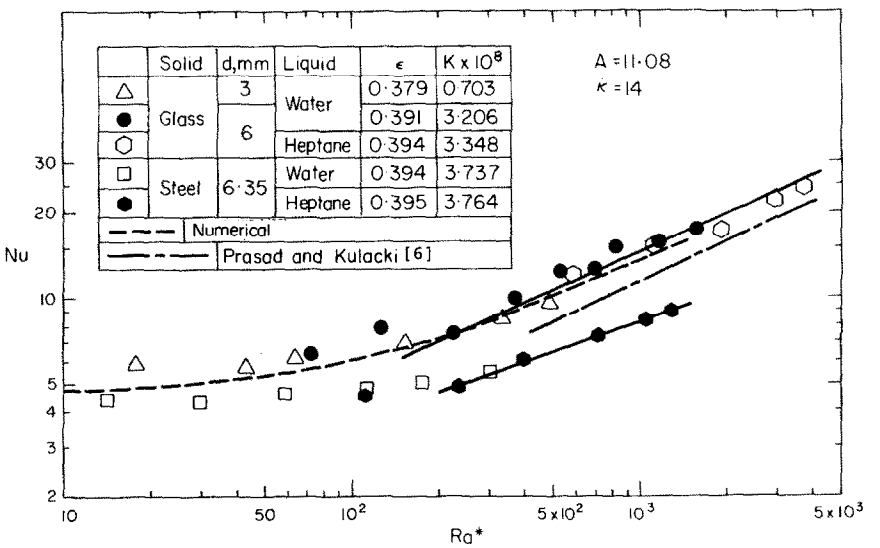

FIG. 5. Heat transfer rates for $A = 11.08$ and $\kappa = 14$ (Rayleigh number based on mean temperature difference).

Nusselt and Rayleigh numbers presented in Figs. 4 and 5 are based on the stagnant thermal conductivity of the porous medium, k_m, obtained from the correlation of Yagi *et al.* [15]. Though it was possible to measure the stagnant thermal conductivity for the test cases 2, 3, 5, 7 and 9 (Table 1), it cannot be measured for the other experiments where the temperature difference of 1°–2°C produces high Rayleigh numbers (out of the conduction regime). Thus, for the internal consistency within all of the present data, k_m was obtained from the correlation for all the test cases.

In Fig. 4a, the experimental results for $\kappa = 3.5$, $A = 14.4$, are presented in terms of the Rayleigh number based on applied heat flux [equation (2)]. In the conduction and asymptotic flow regimes, the experimental data are higher than the theoretical predictions. At low Rayleigh numbers, the difference between the two values is as large as 30%. This difference in experimental and numerical values of Nu is consistent with the temperature distributions on the inner wall. The lower temperatures on the heated wall combined with the sharp rise and fall in the temperature produces a lower mean temperature, $T_{m,i}$, particularly at smaller values of $\overline{Ra^*}$. This results in higher Nusselt numbers.

As the Rayleigh number increases, this difference is observed to decrease, and at high $\overline{Ra^*}$, the experimental values of the Nusselt number for water–glass and heptane–glass closely agree with the numerical predictions. The data for water–steel start diverging for $Ra^* > 300$. In fact, two different curves are followed by the experimental values of Nusselt number, and this has been shown in Fig. 4a by two solid lines. The slopes of the curves for the water–glass and heptane–glass data, and the water–steel data are much different. If an attempt is made to correlate these Nusselt numbers, one obtains

$$Nu = 1.05\,\overline{Ra^*}^{0.18}, \quad 10^2 < \overline{Ra^*} < 10^3 \qquad (6)$$

for the water–steel medium, and

$$Nu = 0.61\,\overline{Ra^*}^{0.30}, \quad 500 < \overline{Ra^*} < 5 \times 10^3 \qquad (7)$$

for the water–glass and heptane–glass media.

The branching behavior of the water–steel data becomes more distinct when the present results are plotted (Fig. 4b) in terms of the Rayleigh number based on the mean temperature difference, Ra^* [equation (4)]. Here, even the heptane–glass data indicate a slight divergence for the present range of Rayleigh number ($Ra^* > 500$). A much larger difference between the water–glass and heptane–glass data has been reported by Prasad *et al.* [8] where the results for both media could be obtained for Ra^* up to 5000. The experimental data of Seki *et al.* [15] for vertical cavities exhibit a similar behavior for ethyl alcohol–glass in comparison to a water–glass medium. An analysis of these results and those for vertical and horizontal cavities [4, 16, 17], and vertical annuli [8], clearly indicates that the Nusselt number for a given Ra^* decreases with an increase in k_s/k_f and vice versa. To draw this conclusion, one can treat water–glass data as reference values for two reasons: (1) k_s/k_f is close to unity; and (2) sufficient results are available in the literature for such a medium. However, when there is a large variation in Prandtl number, this behavior is more complicated owing to the competing effects of the fluid viscosity and conductivity ratio.

Heat transfer rates for $\kappa = 14$ and $A = 11.08$ are presented in Fig. 5, where the Rayleigh number is based on the mean temperature difference. The data for glass–water and glass–heptane exhibit a similar behavior as discussed earlier for $\kappa = 3.5$. A correlation based on these data is obtained as

$$Nu = 0.64\,Ra^{*0.45}, \quad Ra^* > 200 \qquad (8)$$

or

$$Nu = 0.74\,\overline{Ra^*}^{0.31}. \qquad (9)$$

Note that the exponent of the Rayleigh number, $\overline{Ra^*}$, in the present case is very close to that obtained for $\kappa = 3.5$, equation (7).

An interesting aspect of the results presented in Fig. 5 is that the Nusselt numbers for a water–steel medium are much lower than the theoretical predictions, which is not the case for $\kappa = 3.5$ (Fig. 4b). At $\overline{Ra^*} = 15.1$, one will expect a Nusselt number either close to the conduction value or a little higher, but the present value is 16% lower. This behavior of experimental Nusselt number is possible only if a large fraction of power input goes to conduction losses or a higher value of stagnant thermal conductivity is being predicted for the medium. Either of the two will result in lower Nusselt number. It is observed that the amount of conduction loss cannot account for the reduction in Nusselt numbers. One will not obtain a Nu vs Ra^* plot comparable to that plotted in Fig. 4b for water–steel medium even if the heat losses are totally ignored. (We do not expect a completely different behavior for water–steel in the present case when the water–glass and heptane–glass media exhibit a similar trend as observed for $\kappa = 3.5$ in Fig. 4b). It is thus reasonable to assume that the variation in Nusselt number is a result of an improper evaluation of stagnant conductivity, apparently because the correlation of Yagi *et al.* [12] does not properly account for the high permeability near the wall when $r_i \cong d$ and $k_s \gg k_f$.

4.3. *Constant flux vs isothermal heating*

To compare the heat transfer rates for the constant heat flux and isothermal boundary conditions, Nusselt numbers obtained from the correlation of Prasad and Kulacki [6] are plotted along with the present results in Figs. 4b and 5. Compared to the present values for water–glass and heptane–glass media, the Nusselt number for an isothermally heated annulus is 10–30% lower. The difference is smaller at higher Rayleigh numbers, and is observed to increase as Ra^* decreases. Similar behavior is exhibited by the two theoretical results (Fig. 4b). This higher rate of heat transfer for a constant flux boundary condition is consistent with

what has been reported for the vertical cavities [18]. For $\kappa = 14$ and $A = 11.08$ the correlation of Prasad and Kulacki [6] reduces to

$$Nu = 0.44\, Ra^{*0.47}. \quad (10)$$

It can now be observed that the exponents of Ra^* in equations (8) and (10) are close. This agrees with the observation of Prasad and Kulacki [18] that the exponents of Rayleigh number for two types of heating are close to each other in the case of a vertical cavity.

5. CONCLUSION

Free convective heat transfer in a porous, vertical annulus has been experimentally investigated for two sets of aspect and radius ratios, and various solid–fluid combinations. Temperature fields are observed to be strongly influenced by the curvature effects, and the solid–fluid combination, in addition to the Rayleigh number and aspect ratio. The inner wall temperature does not necessarily increase with height. In fact, a sharp rise and fall in temperature takes place depending on the porous medium.

In general, the Nusselt numbers in the present case are higher than those for isothermally heated annuli, and several correlations are presented based on the present experimental data. Furthermore, the Nusselt numbers for various media exhibit a divergent behavior. An analysis of present and previously reported data indicate that the Nusselt number for a given Rayleigh number decreases as k_s/k_f increases and vice versa. The present results further indicate that the theoretical model must be modified to include the channeling effects in the boundary layer, and the effects of the matrix structure and its thermophysical properties.

REFERENCES

1. C. E. Hickox and D. K. Gartling, A numerical study of natural convection in a vertical annular porous layer, ASME Paper No. 82-HT-68 (1982).
2. M. A. Havstad and P. J. Burns, Convective heat transfer in vertical cylindrical annuli filled with a porous medium, *Int. J. Heat Mass Transfer* **25,** 1755–1766 (1982).
3. J. R. Philip, Axisymmetric free convection at small Rayleigh number in porous cavities, *Int. J. Heat Mass Transfer* **25,** 1689–1699 (1982).
4. D. C. Reda, Natural convection experiments in a liquid saturated porous medium bounded by vertical coaxial cylinders, *J. Heat Transfer* **105,** 795–802 (1983).
5. V. Prasad, Natural convection in porous media—an experimental and numerical study for vertical annular and rectangular enclosures, Ph.D. dissertation, University of Delaware (1983).
6. V. Prasad and F. A. Kulacki, Natural convection in a vertical porous annulus, *Int. J. Heat Mass Transfer* **27,** 207–219 (1984).
7. V. Prasad and F. A. Kulacki, Natural convection in porous media bounded by short concentric vertical cylinders, *J. Heat Transfer* **107,** 147–154 (1985).
8. V. Prasad, F. A. Kulacki and M. Keyhani, Natural convection in porous media, *J. Fluid Mech.* **150,** 89–119, (1985).
9. V. Prasad and F. A. Kulacki, Convective heat transfer in a rectangular porous cavity—effect of aspect ratio on flow structure and heat transfer, *J. Heat Transfer* **106,** 158–165 (1984).
10. A. V. Kulkarni, Experimental studies on convective heat transfer in a vertical porous annulus with constant heat flux on the inner wall, M.S. thesis, University of Delaware (1983).
11. J. Bear, *Dynamics of Fluids in Porous Media.* Elsevier, Amsterdam (1972).
12. S. Yagi, D. Kunii and N. Wakao, Radially effective thermal conductivities in packed beds, *Int. Dev. Heat Transfer* 742–749 (1961).
13. Y. Katto and T. Masuoka, Criterion for the onset of convective flow in a porous medium, *Int. J. Heat Mass Transfer* **10,** 297–309 (1967).
14. I. Catton, Natural convection heat transfer in porous media, *Proc. NATO Advanced Study Institute on Natural Convection: Fundamentals and Applications.* Hemisphere, New York (1985).
15. N. Seki, S. Fukusako and H. Inaba, Heat transfer in a confined rectangular cavity packed with porous media, *Int. J. Heat Mass Transfer* **21,** 985–989 (1978).
16. M. Combarnous, Convection naturelle et convection mixte dans une couche poreuse horizontale, *Rev. gen. Thermique* **9,** 1355–1375 (1970).
17. K. J. Schneider, Investigation of the influence of free thermal convection on heat transfer through granular materials, *Progress in Refrigeration Science Technology, Proc. 11th Int. Congress on Refrigeration,* Paper No. II-4, pp. 247–254 (1963).
18. V. Prasad and F. A. Kulacki, Natural convection in a rectangular porous cavity with constant heat flux on one vertical wall, *J. Heat Transfer* **106,** 152–157 (1984).

CONVECTION NATURELLE DANS UN ESPACE ANNULAIRE POREUX VERTICAL AVEC FLUX DE CHALEUR UNIFORME SUR LA PAROI INTERNE—RESULTATS EXPERIMETAUX

Résumé—On étudie la convection naturelle permanente dans un espace annulaire vertical, empli d'un milieu poreux saturé, avec la paroi externe isotherme froide. Les profils de température et les flux sont obtenus pour deux couples de rapports de forme et de rayon, $A = 14{,}4$, $\kappa = 3{,}5$ et $A = 11{,}08$, $\kappa = 14$. L'utilisation de plusieurs combinaisons solide–fluide indique un comportement divergent des courbes du nombre de Nusselt fonction du nombre de Rayleigh, déjà rapporté par d'autres auteurs. Une analyse des données expérimentales montre que le nombre de Nusselt pour un nombre de Rayleigh donné décroit quand le rapport des conductivités du solide et de fluide augmente et réciproquement.

FREIE KONVEKTION IN EINEM VERTIKALEN PORÖSEN RINGSPALT MIT KONSTANTEM WÄRMESTROM AN DER INNEREN WAND

Zusammenfassung—Die stationäre natürliche Konvektion in einem schlanken, vertikalen, konzentrischen Ringspalt, der mit gesättigtem porösem Material gefüllt war, wurde experimentell für den Fall untersucht, daß die innere Wand durch einen aufgeprägten konstanten Wärmestrom beheizt und die äußere Wand isotherm gekühlt wird. Für zwei unterschiedliche Verhältnisse von Spalthöhe zu -breite und zwei Durchmesser-Verhältnisse, $A = 14{,}4$, $\kappa = 3{,}5$ und $A = 11{,}08$, $\kappa = 14$, wurden Temperaturverläufe und Wärmeübergangs-Koeffizienten ermittelt. Der Einsatz von verschiedenen Feststoff–Fluid Kombinationen brachte, wie schon von anderen Autoren berichtet, ein unterschiedliches Verhalten der Kurven $Nu = f(Re)$. Eine nähere Untersuchung der vorliegenden und früheren experimentellen Daten zeigte, daß die Nusselt-Zahl für eine gegebene Rayleigh–Zahl abnimmt, wenn das Verhältnis der Wärmeleitfähigkeiten von Feststoff und Fluid zunimmt und umgekehrt.

СВОБОДНАЯ КОНВЕКЦИЯ В ВЕРТИКАЛЬНОМ ПОРИСТОМ КОЛЬЦЕВОМ ЗАЗОРЕ С ПОСТОЯННЫМ ПОТОКОМ ТЕПЛА НА ВНУТРЕННЕЙ СТЕНКЕ. РЕЗУЛЬТАТЫ ЭКСПЕРИМЕНТА

Аннотация—Экспериментально исследуется установившаяся естественная конвекция в концентрическом вертикальном кольцевом зазоре большой высоты, заполненном насыщенной пористой средой, причем внутренняя стенка нагревается постоянным тепловым потоком, а наружная охлаждается изотермически. Профили температуры и скорости теплопереноса получены для двух значений отношений сторон и радиусов $A = 14{,}4$; $K = 3{,}5$ и $A = 11{,}8$; $K = 14$. Использование различных комбинаций твердое тело–жидкость показывает различное поведение зависимости числа Нуссельта от числа Рэлея, что также подтверждается работами других авторов. Анализ полученных в работе и ранее опубликованных экспериментальных данных показывает, что для данного числа Рэлея число Нуссельта уменьшается с ростом отношения удельных теплопроводностей твердого тела и жидкости, и наоборот.